

Low-Profile Interconnects via Laser-Induced Forward Transfer

Kristin M. Charipar, Nicholas A. Charipar, Raymond C.Y. Auyeung, Heungsoo Kim and Alberto Piqué

*Naval Research Laboratory, Materials Science & Technology Division,
4555 Overlook Ave. SW, Washington, DC 20375, USA
E-mail: kristin.charipar@nrl.navy.mil*

Direct-write processes offer several advantages over traditional lithographic techniques, including high processing speeds, high resolution, and the ability to fabricate complex 2D and 3D structures. Specifically, laser-induced forward transfer (LIFT) is a non-lithographic process that can be utilized to efficiently print numerous materials on various substrates with high precision. By using high viscosity nanopastes, structures can be printed with high positional accuracy that maintain the shape of the spatially structured laser beam. This capability lends itself to applications such as sensors and microelectronic components requiring features with narrow pitch. Because of the versatility of the LIFT process, interconnects can be printed directly onto the bond pads of both flip-chip devices in addition to directly onto substrates. In this work, we demonstrate the use of LIFT for printing high-aspect ratio vertical micro-pillars combined with freestanding voxels to fabricate low profile interconnects on a bare die LED.

DOI: 10.2961/jlmn.2018.02.0003

Keywords: bare die, interconnects, laser-induced forward transfer (LIFT), laser processing, surface mounting

1. Introduction

Direct-write techniques have been developed over the past few decades to meet the demand for printing functional materials [1]. These methods are non-contact and do not rely on traditional photolithography, making them lower cost, simpler to implement, and more environmentally friendly. Most direct-write techniques are based on the principle of dispensing, such as inkjet [2,3], or printing discrete voxels of various materials onto substrates. Inkjet processes rely on dispensing materials through nozzles, which limits the range of viscosities that are compatible with printing.

While most direct-write methods are confined to two dimensions, fabrication of 3D microstructures are enabled by laser-induced forward transfer, or LIFT. This laser-based printing process involves the ejection of material from a donor substrate, or “ribbon”, onto a closely-positioned receiving substrate through the application of a laser pulse. The laser pulse ejects the material without damaging it or the ribbon by vaporizing some fraction of the thin layer of material that is present at the material/substrate interface [4,5]. LIFT is non-contact and nozzle-free which eliminates issues related to nozzle clogging and enables the possibility of using higher viscosity materials. By using a high viscosity nanopaste, both 2D and 3D structures can be built by stacking successive voxels [6], to form freestanding features [7]. By shaping the laser beam with an aperture, the size and shape of the transferred voxel can be precisely controlled.

The LIFT process is compatible with a wide range of materials with high resolution without the need for traditional lithography tools, making it a truly maskless process. In addition, it is uniquely designed for rapid prototyping because designs and printed patterns can be changed quick-

ly, without the need to fabricate a new mask every time a design is altered.

Because LIFT is a versatile tool used to print electronic structures with high precision and speed, it is ideally suited for the fabrication of electrical interconnects [8,9]. By having precise control over the size and shape of the printed voxel, very fine features (a few microns) can be printed. Standard ball bonders used for manufacturing wire bonds typically produce interconnects that are on the order of tens of microns [10]. Additionally, because LIFT can print high resolution features and is a non-contact process, devices can be more tightly packed on circuit boards, reducing the circuit footprint.

In addition, wire bonding produces interconnects that typically add to the overall z-height of the device, whereas laser printed interconnects are essentially flush with the bare die surface. This is an important advantage because it means that vertical integration can be made more efficient in circuit layout, where wire-bonding height limits decrease the number of circuit layers that can be stacked in a device.

In this work, we use LIFT to print low-profile interconnects consisting of micro-pillars combined with freestanding micro-bridges. We demonstrate fully functional laser printed interconnects on a bare die LED. Optical characterization is performed to confirm that the LED was undamaged during the laser printing process, while electrical properties provide I-V curves to give insight into the interconnect performance as compared to wire bonding.

2. Experimental Methods

Laser-induced forward transfer (LIFT) experiments were conducted using a frequency-tripled Nd:YVO₄ pulsed laser (JDSU, Q301-HD, $\lambda = 355$ nm, FWHM = 30 ns) operating at 30 kHz. Laser pulse amplitude and pulse picking were controlled using an acousto-optic modulator (NEOS

Technologies, AOM 35085-3-350). To achieve a uniform laser spot, the beam was shaped through an aperture and subsequently imaged through a 10x objective onto the ribbon. The laser printing process was imaged by an inline CCD camera through the objective to allow for a real-time plan view of the ribbon as seen by the laser beam. Further details regarding the LIFT process can be found in a previous publication [11].

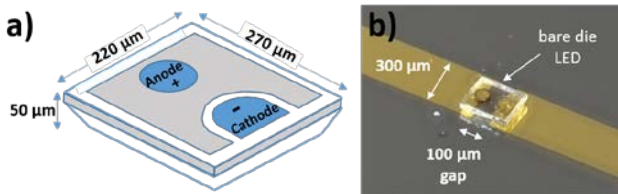


Fig. 1. (a) Schematic of a bare die LED, showing anode and cathode configuration and (b) optical image of the LED mounted onto the test fixture before laser printing interconnects.

The receiving substrate used was a bare die LED (Cree, TR2227-0216) mounted onto a patterned substrate. The LED chosen for this work, which measures $\sim 220 \mu\text{m} \times 270 \mu\text{m}$, can be seen schematically in Fig. 1(a). It contains two top side contacts, where both the anode and cathode (both with a diameter of $\sim 80 \mu\text{m}$) are on the top bare die surface. Test fixtures were fabricated on Au-coated Si substrates, each 1 cm x 1 cm, using standard photolithography methods. The Au feed lines were $300 \mu\text{m}$ wide with a $100 \mu\text{m}$ gap, where the LED is placed. The LED was mounted in the gap (seen in Fig. 1(b)) using an adhesive (VPG, M-Bond 610) via an SMD rework station (PACE Worldwide, TF1800). The test fixture was then cured in an oven at 125°C for 1 hour to harden the adhesive.

For this work, the material used to print the interconnects was a high-viscosity Ag nanopaste [12] (Harima Chemicals Group, NPS, viscosity $\sim 100\text{Pa}\cdot\text{s}$, 80wt% solids loading). The ribbon was prepared by doctor blading the nanopaste into $8 \mu\text{m}$ deep wells in a glass substrate. The ribbons were stored in a nitrogen desiccator to prevent oxidation of the Ag surface and also to remove some of the volatiles to tailor the viscosity of the transferred material to produce optimal congruent voxels [13].

The receiving substrate, consisting of the test fixture, was placed onto a carrier wafer via semiconductor dicing tape. A combination of Si wafer and Kapton spacers similar in thickness to the receiving substrate plus the thickness of the bare die LED ($\sim 550 \mu\text{m}$) were used to ensure a small gap ($\sim 25 \mu\text{m}$) between the ribbon and receiving substrate (LED). The carrier wafer was held in place via a vacuum chuck that was mounted on top of computer-controlled x-y translation stages (Aerotech, ALS50100 / ALS50045).

A schematic of the laser printing process can be seen in Fig. 2, where it is shown that the interconnects are fabricated via a two-step process, where micro-pillars are first printed, followed by a free-standing bridge to connect the micro-pillar to the LED bond pads. Laser printing was performed using square voxels, $\sim 75 \mu\text{m} \times 75 \mu\text{m}$, with a laser fluence of $\sim 50\text{-}100 \text{ mJ}/\text{cm}^2$, to fabricate the micro-pillars onto the substrate. Because the printing material has a sufficiently high viscosity, the voxels were stacked on top of

one another to build the micro-pillar in the z-direction. Then, a rectangular voxel, $\sim 75 \mu\text{m} \times 200 \mu\text{m}$, was used to fabricate the micro-bridge between the top micro-pillar surface and the LED cathode and anode bond pads.

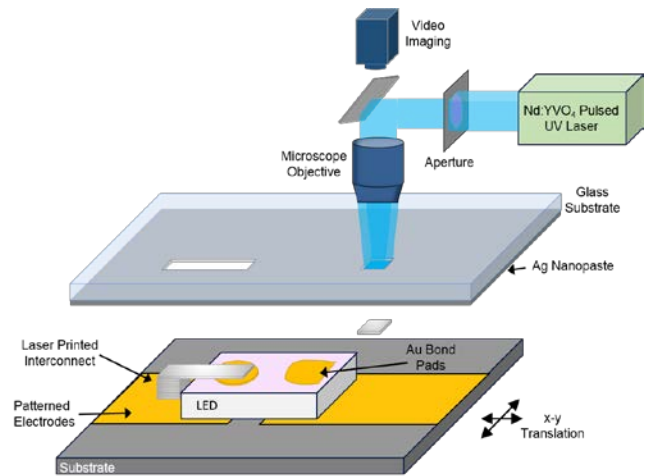


Fig. 2. Schematic of laser-induced forward transfer (LIFT) of interconnects onto an LED.

After laser printing, the interconnects were cured in an oven at 125°C for 45 min and then characterized via optical microscopy using a bright-field optical microscope (Keyence, VHX-1000). Laser printed 3D structures were also imaged using a scanning electron microscope (JEOL, JSM-7001F). To confirm that the LED did not undergo any degradation during the laser printing process, the optical properties of the LED were characterized using a spectrometer with an integrating sphere (Ocean Optics, ISP-50-8-R). Silver epoxy (Epoxy Technology Inc., EPO-TEK H20E) was used to attach leads to the test fixture for electrical characterization via a sourcemeter (Keithley, 2400).

3. Results & Discussion

Using LIFT to print interconnects offers several advantages over traditional wire-bonding techniques. First, laser printing offers high speeds, where interconnects can be printed using galvanometric scanning mirrors of up to 1 m/s. While this process is still serial in nature, similar to wire-bonding, it is potentially faster as ball bonders can produce ~ 10 wires/s in a high-throughput manufacturing environment [14]. In addition, to scale up the process from using a single ribbon with material, a roll-to-roll process could be implemented as a means of continually providing new material for printing.

Typical wirebonding equipment relies on thermocompression or ultrasonic bonding to produce interconnects, which is inherently a contact process. Alternatively, laser printing is non-contact and can be used to fabricate interconnects on delicate bare die because the only force that is applied during processing comes from the weight of transferred material landing on the bond pad surface. However, because wire bonders use ultrasonic energy to create wire-bonds, metallic bonds can be formed at the interface between the bond pad and interconnect material, which is typically Au or Cu. This is important because the creation

of metallic bonding at the interface ensures low contact resistance and improved electrical performance [15]. While laser printing interconnects does not inherently produce these desired interfaces, the resistivity of laser printed Ag interconnects after thermal cure at 150°C can reach as low as $\sim 4x$ that of bulk Ag [6].

In addition, it is possible to print different materials using LIFT, where the conductivity can be tailored based on materials properties. By using high-viscosity nanopaste, the size and shape of the transferred voxel can be precisely controlled by choosing the shape and size of the aperture that is used to shape the laser beam. Thus, very small (a few microns) features can be printed, allowing interconnects to be fabricated on bare die that are closer together than wire-bonding would allow. This means that the overall circuit footprint is reduced, allowing for more devices to fit into a fixed area. By printing congruent voxels out-of-plane, low-profile interconnects are made possible without the need for wire-bonding equipment.

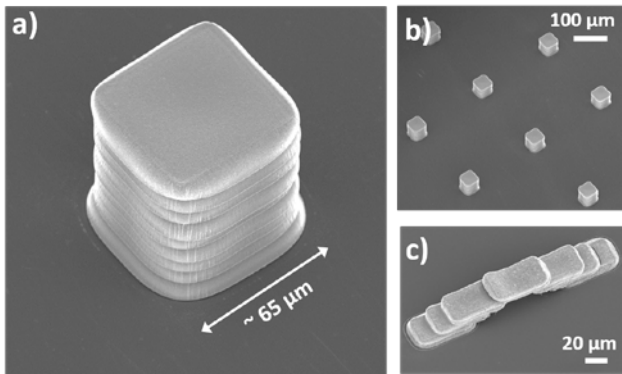


Fig. 3. Scanning electron micrographs of laser printed (a) micro-pillar ($\sim 65 \mu\text{m} \times 65 \mu\text{m}$), (b) micro-pillar arrays and (c) freestanding 'staircase' structure (individual voxels $\sim 30 \mu\text{m} \times 70 \mu\text{m}$).

The ribbon used as the donor substrate contained 8 μm deep lithographically patterned wells on a glass substrate. After doctor blading, the Ag nanopaste layer produces transfers that are $\sim 6 \mu\text{m}$ thick before thermal curing. Because the LED is $\sim 50 \mu\text{m}$ thick, nine successive voxels were printed to produce a micro-pillar of an appropriate height to interconnect to the bare die bond pad. A scanning electron micrograph of a laser printed micro-pillar ($\sim 65 \mu\text{m} \times 65 \mu\text{m}$) can be seen in Fig. 3(a). This image highlights the ability of LIFT to fabricate out-of-plane structures by stacking successive congruent voxels. In addition, an array of micro-pillars is seen in Fig. 3(b), where it is clear that 3D structures can be printed with high lateral precision and repeatability. Because of the versatility of the LIFT process, any size and shape voxel can be printed by adjusting the aperture used to shape the laser beam [16]. To demonstrate that rectangular voxels can be printed to create the second part of the wire-bond-like structure, a staircase was printed, where the top voxels are freestanding without support underneath (seen in Fig. 3(c)).

Because the cathode and anode bond pads on the LED are both $\sim 80 \mu\text{m} \times 80 \mu\text{m}$ in size, a similarly sized voxel ($\sim 75 \mu\text{m}$ square) was chosen to fabricate the micro-pillars. To connect the micro-pillars to the top side contacts, free-

standing micro-bridges, measuring $\sim 75 \mu\text{m} \times 200 \mu\text{m}$, were printed using a rectangular aperture.

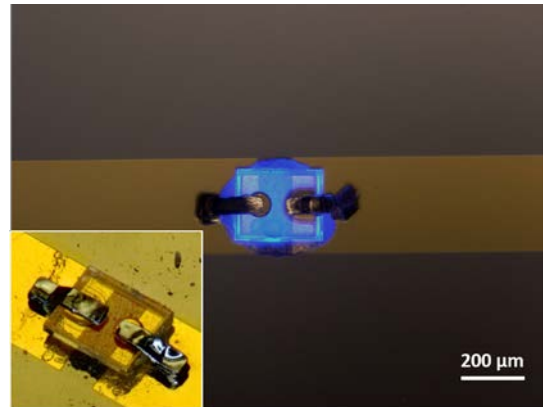


Fig. 4. Optical micrograph of LED operating at 1 mA. Inset: At-an-angle micrograph view of laser printed interconnects, including micro-pillar with freestanding bridge onto LED bond pad.

An optical image of the LED with laser printed interconnects operating at forward current, $I_f = 1 \text{ mA}$ can be seen in Fig. 4. Operation of the LED at $I_f = 20 \text{ mA}$, the maximum operating current, was too bright to capture the fine details of the device and test fixture in an optical image. The interconnects show some degree of shrinkage during cure which can be seen in the inset of Fig. 4. The laser printed micro-bridges are bent slightly down off of the surface of the LED to meet the micro-pillars. After curing the individual printed voxel height is $\sim 4 \mu\text{m}$, which equates roughly to a shrinkage factor of $\sim 35\%$. The height of the printed micro-pillars can be adjusted to compensate for any shrinkage related to curing. In a previous study, we have shown that interconnects can be conformally printed over 3D surfaces [9]. However, the voxels can become stressed during certain curing conditions which can lead to cracking and failure at the curved portions of the interconnect. By printing interconnects in a two-step process, where the height of the micro-pillars is tailored specifically to the height of the bare die interconnect, stress can be relieved, reducing the possibility of cracking.

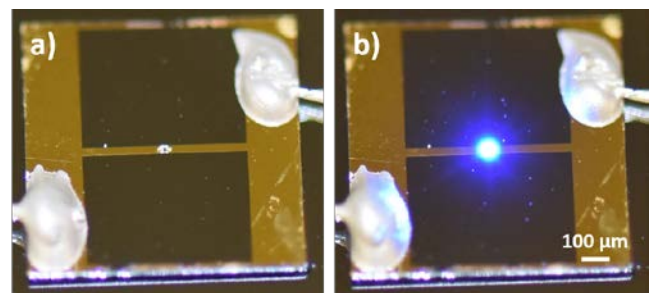


Fig. 5. Optical micrographs of bare die LED mounted on patterned electrodes with laser printed interconnects at (a) $I_f = 0 \text{ mA}$ and (b) $I_f = 5 \text{ mA}$.

In addition, it is possible to cure the nanopaste using a reflow oven, which provides a rapid, high temperature anneal that does not degrade the bare die performance and minimizes voxel shrinkage [17]. The test fixture, which measures 1 cm x 1 cm, with an LED and laser printed in-

terconnects can be seen in Fig. 5(a), where the LED, operating at $I_f = 5$ mA, can be seen in Fig. 5(b).

To determine the functionality of the laser printed interconnects compared to the bare die specifications, I-V measurements were taken from $I_f = 100$ μ A to 18 mA. The curve, seen in Fig. 6, shows a forward voltage of ~ 3.5 V at 18 mA, which closely matches that of the manufacturer's specifications, which states a nominal forward voltage of ~ 3.3 V. The small discrepancy in forward voltage can be attributed to device variation and is consistent with InGaN-based diodes. These observations confirm that the laser printed interconnects perform as well as wire-bonded interconnects via the bare die specifications.

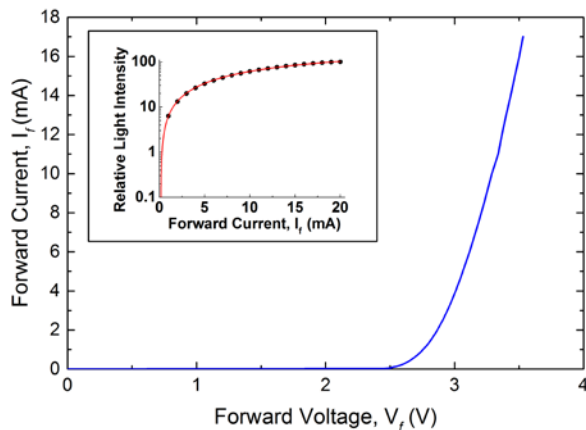


Fig. 6. Forward current as a function of forward voltage, indicating a nominal operating voltage of ~ 3.5 V. *Inset:* Relative light intensity as a function of forward operating current (black circles), with exponential fit (red line).

In addition to characterization of electrical properties of the LED, the optical properties were measured using a spectrometer. Individual emission spectra were collected at varying currents, starting at 1 mA and up through 20 mA, at 1 mA intervals. The light intensity outputs were normalized to 20 mA as a maximum reference. The normalized peak of each spectra as a function of forward current can be seen in the Fig. 6 inset, where the black circles indicate collected data points and the red line is a closely matched exponential fit of the data.

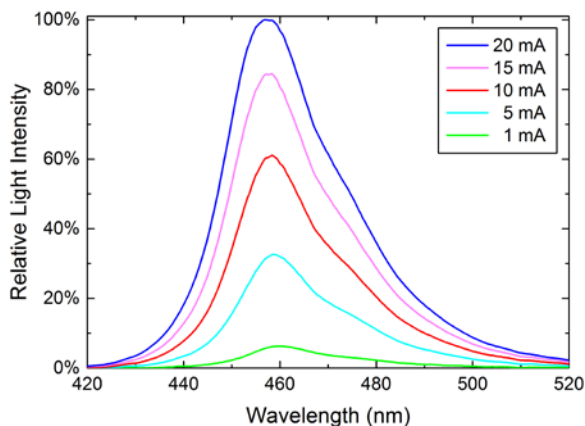


Fig. 7. Emission spectra as function of wavelength for varying operating current.

The light intensity profiles at various operating currents can be seen in Fig. 7, where the spectra are also normalized to the maximum operating current of 20 mA. In addition, a subtle spectral shift is observed as the operating current is increased, where the spectral peak is shifted by ~ 2 nm from 460.4 nm at 1 mA to 457.8 nm at 20 mA. This data confirm that the laser printed interconnects are of high quality with low contact resistance and LIFT fabrication and subsequent thermal curing did not degrade the LED functionality.

4. Conclusion

Low profile interconnects on LEDs were fabricated via laser-induced forward transfer. The electrical and optical properties were characterized and show that the I-V curve matches that of the LED specifications and the LED was undamaged during processing. Laser printing offers the flexibility of materials choices and enables the fabrication of both 2D and 3D microstructures, including electrical interconnects.

Acknowledgments

This work was funded by the Office of Naval Research (ONR) through the Naval Research Laboratory Basic Research Program.

References

- [1] A. Piqué and D.B. Chrisey: "Direct-Write Technologies for Rapid Prototyping Applications" (Academic Press, San Diego, 2002).
- [2] P. Calvert: Chem. Mater., 13, (2001) 3299.
- [3] D. Soltman, B. Smith, H. Kang, S.J.S. Morris, and V. Subramanian: Langmuir, 26, (2010) 15686.
- [4] C. Boutopoulos, A.P. Alloncle, I. Zergioti, and P. Delaporte: Appl. Surf. Sci., 257, (2013) 71.
- [5] M. Duocastella, A. Patrascioiu, V. Dinca, J.M. Fernandez-Pradas, J.L. Morenza, and P. Serra: Appl. Surf. Sci., 257, (2011) 5255.
- [6] J. Wang, R.C.Y. Auyeung, H. Kim, N.A. Charipar, and A. Piqué: Adv. Mat., 22, (2010) 4462.
- [7] R.C.Y. Auyeung, H. Kim, A.J. Birnbaum, M. Zalalutdinov, S.A. Mathews, and A. Piqué: Appl. Phys. A, 97, (2009) 513.
- [8] E. Breckenfeld, H. Kim, R.C.Y. Auyeung, N. Charipar, P. Serra, and A. Piqué: Appl. Surf. Sci., 331, (2015) 254.
- [9] H. Kim, M. Duocastella, K.M. Charipar, R.C.Y. Auyeung, and A. Piqué: Appl. Phys. A, 113, (2013) 5.
- [10] T. Tekin: IEEE J. Sel. Top. Quant. Electr., 17, (2011) 704.
- [11] S.A. Mathews, R.C.Y. Auyeung, H. Kim, N.A. Charipar, and A. Piqué: J. Appl. Phys., 114, (2013) 064910-1-10.
- [12] Harima Chemicals Inc. <http://harimatec.com/products/conductive-paste/> (2018).
- [13] A. Piqué, H. Kim, R.C.Y. Auyeung, I. Beniam, and E. Breckenfeld: Appl. Surf. Sci., 374, (2016) 42.
- [14] G. Harman: "Wire Bonding in Microelectronics" (McGraw Hill, New York, 2010).
- [15] H. Xu, V.L. Acoff, C. Liu, V.V. Silberschmidt, and Z. Chen: Microelectr. Eng., 88, (2011) 3155.

- [16] K.M. Charipar, R.E. Díaz-Rivera, N.A. Charipar, and A. Piqué: Proc. SPIE, (2018)105230R.
- [17] K.M. Charipar, N.A. Charipar, J.C. Prestigiacomo, N.S. Bingham, and A. Piqué: J. Manuf. Proc., 32, (2018) 110.

(Received: June 23, 2018, Accepted: August 25, 2018)